JCTC Journal of Chemical Theory and Computation

Development and Validation of the B3LYP/N07D Computational Model for Structural Parameter and Magnetic Tensors of Large Free Radicals

Vincenzo Barone,* Paola Cimino,[+] and Emiliano Stendardo

LSDM and INSTM-Village, Dipartimento di Chimica 'Paolo Corradini', Complesso Universitario Monte S. Angelo, via Cintia, I-80126 Napoli, Italy

Received January 31, 2008

Abstract: Extensive calculations on a large set of free radicals containing atoms of the second and third row show that the B3LYP/N07D computational model provides remarkably accurate structural parameters and magnetic tensors at reasonable computational costs. The key of this success is the optimization of core-valence *s* functions for hyperfine coupling constants, while retaining (and even improving) the good performances of the parent 6−31+G(d,p) basis set for valence properties through reoptimization of polarization and diffuse *p* functions.

Introduction

Quantum mechanical treatments of interactions between atomic and molecular systems have provided an invaluable contribution toward a deeper understanding of the interplay between different factors in determining structures, binding energies, and physicochemical properties of noncovalently bonded complexes.[1,2] While very reliable static properties of small and medium size systems can be safely computed by state of the art post-Hartree–Fock methods,[3,4] the situation is more involved for large systems in condensed phases[5] and whenever dynamical aspects cannot be neglected.[6] The development of reliable density functionals (especially hybrid ones),[7–10] mixed discrete/continuum solvent models,[11,12] and implementation of linear scaling computational approaches[13] is allowing the reliable study of large systems of biological and technological relevance.[14] However, the problem of basis set superposition error (BSSE) and of the computation of reliable electric and magnetic properties by basis sets of nonprohibitive dimensions remains open.[15,16] This is even more important in the framework of ab initio dynamics[17,18] where a huge number of different structures (and energy gradients) must be computed to produce a converged trajectory.[19,20] Several recent studies have shown that in the framework of hybrid density functionals and ab initio dynamics, the smallest basis sets allowing semiquantitative evaluations without too large errors connected to basis set incompleteness are split valence sets augmented by diffuse functions.[21,22] Among those, aug-cc-pVDZ[23] and 6–31+G(d,p)[24] models lead to comparable results. From a complementary point of view, the same level of basis sets allows for the computation of reasonable electric and magnetic properties, except for hyperfine coupling constants, which require specialized functions in the core-valence region.[25,26]

All these considerations prompted us to optimize a new polarized split-valence basis set for second- and third-row atoms, which, adding a reduced number of polarization and diffuse functions to the 6–31G set, leads to an optimum

Table 1. Basis Functions To Be Added to 6-31G for Obtaining the N07D Basis Set for the B3LYP Functional[a]

	s	*p*	*d*	*d*
H		0.750		
B		0.035	0.343	
C	7.5	0.050	0.820	
N	12.6	0.053	1.015	
O	15.1	0.065	1.190	0.180
F	18.3	0.083	1.370	0.230
Al	3.1	0.015	0.189	
Si	3.6	0.033	0.275	
P	5.5	0.035	0.373	
S	8.0	0.041	0.479	
Cl	8.5	0.048	0.600	0.196

[a] For He, Li, Be, Na, and Mg atoms N07D is identical to 6-31+G(d,p).

* Corresponding author e-mail: baronev@unina.it.

[+] Permanent address: Dipartimento di Scienze Farmaceutiche, Università di Salerno, via Ponte don Melillo, I-84084 Fisciano (Sa), Italy.

10.1021/ct800034c CCC: $40.75
Published on Web 04/09/2008

Table 2. Comparison of Parameters for HF, HCl, H_2O and TEMPO Calculated by Different Basis Sets

	H_2O			HF		HCl		TEMPO	
	OH (Å)	HOH (degrees)	μ (Debye)	HF (Å)	μ (Debye)	HCl (Å)	μ (Debye)	NO (Å)	μ (Debye)
6–31G(d)	0.968	103.7	2.094	0.934	1.860	1.289	1.468	1.286	2.894
aug-cc-pVDZ	0.965	104.7	1.854	0.926	1.803	1.295	1.154	1.283	3.122
6–311+G(2d,2p)	0.961	105.1	1.960	0.922	1.882	1.280	1.174	1.281	3.149
N07D	0.964	104.5	1.846	0.925	1.810	1.291	1.181	1.281	3.162
N07D[a]	0.963	105.3	2.114	0.925	1.986	1.291	1.365	1.281	3.215
exp	0.958[b]	104.5[c]	1.855[d]	0.920[d]	1.826[e]	1.275[f]	1.093[f]		

[a] Without diffuse functions on O, F, and Cl atoms. [b] Reference 52. [c] Reference 53. [d] Reference 54. [e] Reference 55. [f] Reference 56.

Table 3. Theoretical and Experimental Hyperfine Coupling Constants (in Gauss) of B, Be, and Cl Atoms[b]

structure	atom	6–31G(d)	EPR-II	EPR-III	N07D	exp[a]
$BO^{\bullet}$	B	376.0	399.3	384.7	375.9	365.7
$BB^{\bullet\bullet}$	B	9.4	4.7	5.5	8.1	5.4
$BS^{\bullet}$	B	289.6			299.6	292.0
$BH_2^{\bullet}$	B	140.9	133.3	129.1	140.2	127.7
$BH_2O^{\bullet}$	B	−26.7	−28.4	−26.7	−28.0	30.0
$BeH^{\bullet}$	Be	−74.2			−70.4	71.1
$BeOH^{\bullet}$	Be	−106.0			−100.6	94.2
$BeF^{\bullet}$	Be	−111.4			−107.4	104.9
$Cl_2^{-\bullet}$	2Cl	27.1			27.7	38.9
$SiCl_3^{\bullet}$	3Cl	9.2			10.7	12.4
$SiCl_2CH_3^{\bullet}$	2Cl	−7.5			−8.6	10.5
$PCl_2^{\bullet}$	2Cl	−2.3			−2.5	0.4

[a] Data for BO, BB, BS, BH_2, BH_2O, BeH, BeOH, BeF, and Cl_2^- are from ref 44; data for $SiCl_3$, $SiCl_2CH_3$, and PCl_2 are from ref 45. [b] All the theoretical values have been obtained in the present work.

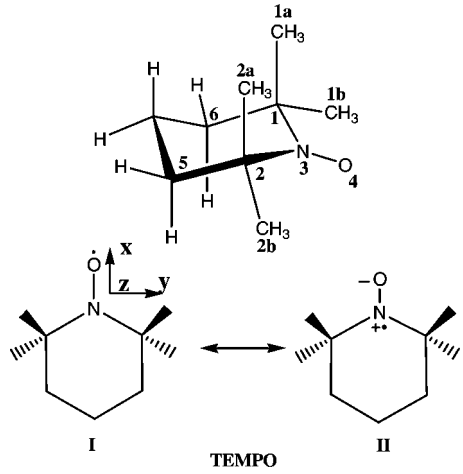

Figure 1. Structure of TEMPO (2,2,6,6-tetramethylpiperidine-*N*-oxyl) radical.

compromise between reliability and computer time. The possible use of different basis sets on different atoms requires basis set balance in order to avoid inaccuracies in the charge distribution of the molecule. For example, adding diffuse functions to split-valence basis sets has a significant effect on the energy even for atoms. Thus, diffuse *p* functions should be added consistently on all non-hydrogen atoms. At the same time, diffuse *s* functions play a negligible role in determining molecular properties and have been neglected for all atoms. The situation is more involved for diffuse *d* functions. Although they have a comparatively lower effect on energies, their role becomes significant for electric properties of electronegative atoms and for some geometrical parameters involving multiple bonds.[27,28] At the same time they adversely affect the basis set superposition error in weak intermolecular interactions. In the present context, diffuse *d* functions have been optimized for all non-hydrogen atoms, but they are systematically used only for some electronegative atoms.

As mentioned above, in the context of magnetic properties, isotropic hyperfine couplings play a peculiar role since their evaluation is quite straightforward, but reliable results can be obtained only by proper inclusion of electron correlation and improved description of core-valence regions.[29–31]

Methods based on the unrestricted Kohn–Sham (UKS) approach to density functional theory (DFT) have revolutionized also this field in the past few years, since some functionals (especially hybrid ones) provide, at least for systems containing only second- and third-row atoms, remarkable results at reasonable costs.[32–37] The basis set issue remains, however, significant.[32] Our experience in developing purposely tailored basis sets indicates that addition of a single core-valence *s* function with an optimized exponent around 10 performs remarkably well.[38,39] The price to be paid for this effective approach is that the basis function must be optimized for each atom and for each different density functional. This is quite disappointing since the remaining part of the basis set can be transferred without modifications among different hybrid density functionals. We have decided, however, that efficiency merits this slight additional effort, and we have optimized semicore *s* functions for several functionals.[40] In the present paper, we will be concerned with the B3LYP functional[41] in view of its widespread use and availability in most computational codes. The functions added to the 6–31G set for all the atoms of the second and third row are shown in Table 1.

The N07D basis set has been already used with success in some structural and dynamic studies both in gas phase

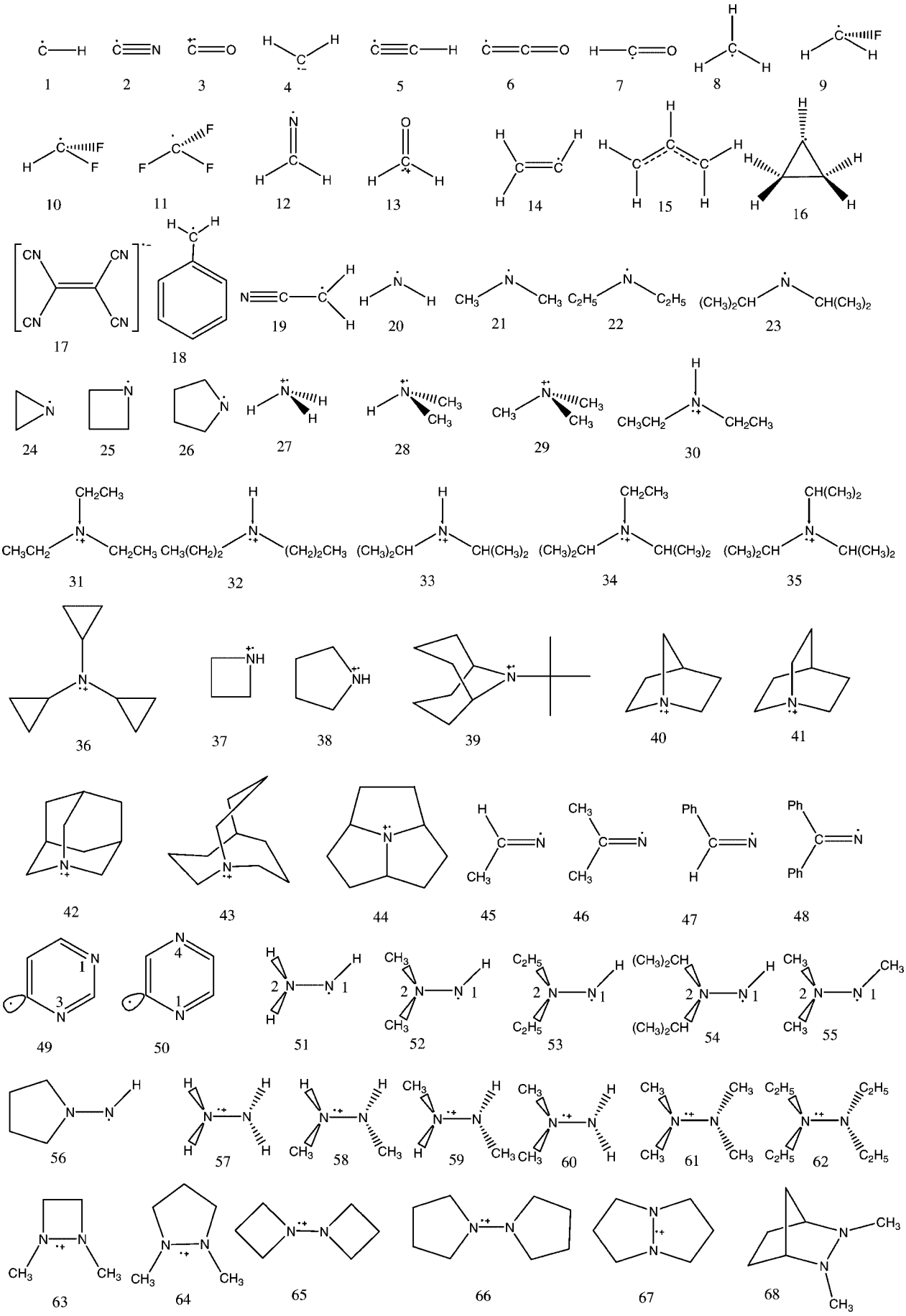

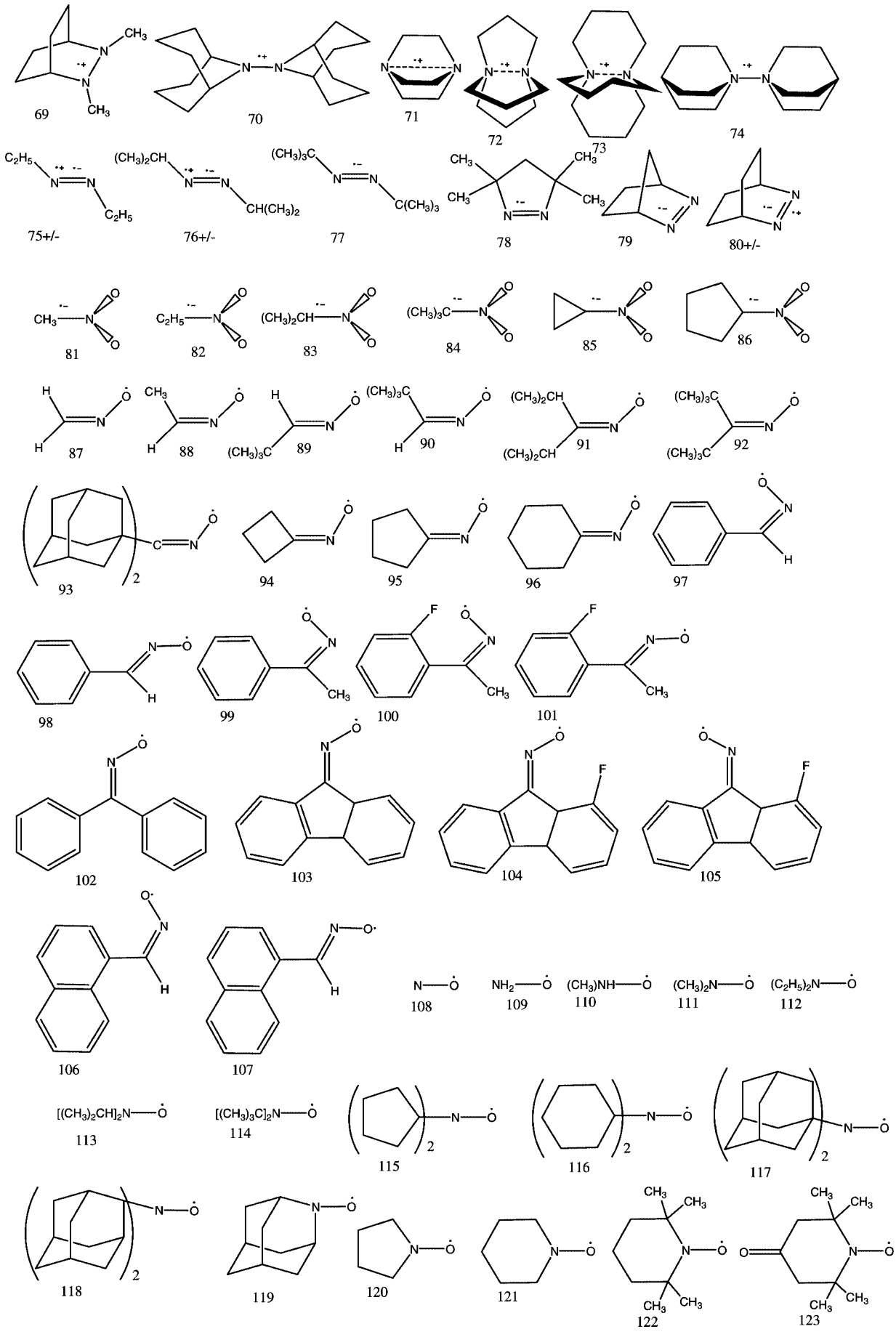
69
70
71
72
73
74
75+/-
76+/-
77
78
79
80+/-
81
82
83
84
85
86
87
88
89
90
91
92
93
94
95
96
97
98
99
100
101
102
103
104
105
106
107
108
109
110
111
112
113
114
115
116
117
118
119
120
121
122
123

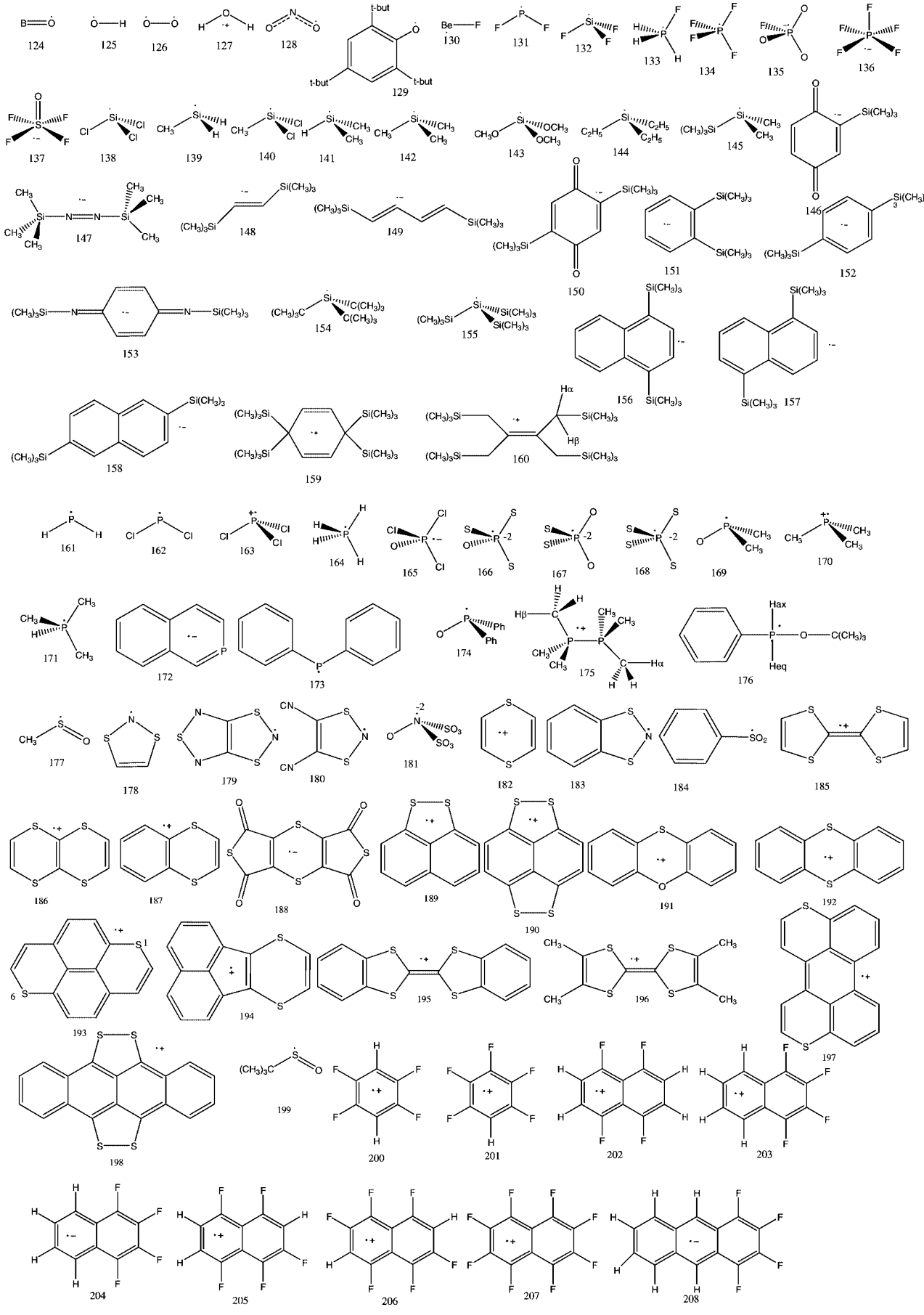

Figure 2. Structures of the radicals studied.

Table 4. Theoretical and Experimental Hyperfine Coupling Constants (Gauss) of Hydrogen Nuclei of the Radicals Studied[b]

		6–31G(d)	EPR-II	EPR-III	N07D	exp[a]
1	H	−18.2	−17.8	−17.1	−17.0	20.6
4	2H	−17.1	−16.8	−13.8	−14.2	16.0
5	H	21.8	21.9	21.1	21.8	18.0
8	3H	−25.2	−23.8	−23.2	−23.0	25.0
9	2H	−18.3	−17.8	−17.6	−17.4	21.1
10	H	−23.1	−24.5	−25.3	−22.1	22.2
12	H	−78.8	−83.4	−83.0	−79.4	83.2
13	2H	−121.5	−128.2	−128.7	−120.0	132.7
14	Hcis	59.8	63.8	63.8	59.5	68.5
14	Htrans	36.6	40.2	40.2	36.0	34.2
14	H(CH)	14.0	17.1	17.5	13.9	13.3
15	2Hcis	−15.8	−14.9	−14.5	−14.3	13.5
15	2Htrans	−16.5	−15.7	−15.4	−15.0	14.8
15	H(CH)	4.9	4.7	4.5	4.4	4.2
18	H(orto)	−6.0	−5.8	−5.6	−5.9	5.2
18	H(meta)	2.6	2.5	2.4	2.5	1.8
18	H(para)	−6.8	−6.6	−6.5	−6.7	6.2
18	H(CH2)	−18.3	−17.4	−16.8	−17.6	16.3
125	H	−24.2	−24.0	−23.7	−23.4	25.5
127	H	−24.9	−25.6	−25.3	−24.7	26.1
130	2H	−13.6	0.0	0.0	−13.8	11.8
202	4H	−2.0	−2.0	−1.9	−2.0	4.0
203	2H	−5.1	−4.9	−4.9	−5.1	2.4
203	2H	−1.2	−1.2	−1.2	−1.2	0.6
204	2H	−7.3	−6.8	−6.7	−7.1	5.6
204	2H	−2.1	−2.0	−2.0	−2.1	1.4
205	H	−1.1	−1.1	−1.1	−1.1	2.1
205	H	−3.1	−2.9	−2.9	−3.0	4.2
206	2H	−0.1	−0.1	−0.1	−0.1	0.3

[a] Experimental data for 1, 4, 5, 8–10, 12–15, and 18 are from ref 44; for 203–207 are from ref 55. [b] All the theoretical values have been obtained in the present work.

Table 5. Data Analysis for Hydrogen Nuclei[a]

	6–31G(d)	EPR-II	EPR-III	NO7D	exp
		Hydrogen: $N = 29$			
MAD	2.1	1.8	1.9	1.8	
max absolute error	11.3	6.0	6.0	9.0	
average *E*%	25.3%	25.4%	25.4%	25.9%	
max *E*%	113.1%	108.4%	104.6%	113.9%	
R2	0.9946	0.9938	0.9934	0.9943	
intercept	1.4936	0.8670	0.5675	1.0527	
slope	0.9097	0.9666	0.9691	0.9051	
max	121.5	128.2	128.7	120.0	132.7
min	0.1	0.1	0.1	0.1	1.8

[a] MAD (mean absolute deviation in Gauss) $= \Sigma|a_{calc} - a_{exp}|/N$; *E*% (percent error) $= a_{calc} - a_{exp}/a_{exp}$.

Table 6. Theoretical and Experimental Hyperfine Coupling Constants (Gauss) of Carbon Nuclei

structure	carbon (^{13}C)	6–31G(d)[a]	EPR-III[a]	TZVP[a]	cc-pVQZ[a]	N07D[b]	exp[a]
1	C	16.8	19.0	14.8	9.0	15.5	16.8
2	C	183.9	207.7	214.6	201.6	200.9	209.8
3	C	495.3	569.3	587.8	566.5	555.3	561.3
4	C	33.0	29.4	20.7	16.0	27.3	21.0
5	C	348.2	378.7	390.7	374.3	371.3	362.0
5	C(H)	72.9	81.2	82.9	83.5	78.9	76.0
6	C	16.7	14.2	12.0	8.1	13.3	15.7
6	C(O)	−2.7	−7.1	−8.5	−8.1	−6.5	10.7
7	C	152.2	138.5	142.7	136.8	137.1	134.7
8	C	44.4	28.6	27.0	19.9	28.7	27.0
9	C	62.3	56.4	50.9	40.0	56.3	54.8
10	C	152.8	143.4	146.8	137.6	145.4	148.8
11	C	258.9	264.5	274.0	261.3	266.9	271.6
12	C	−23.6	−24.5	−25.7	−24.4	−24.4	28.9
13	C	−30.1	−33.5	−35.1	−33.2	−33.2	38.9
14	C	121.9	107.7	109.6	101.5	109.5	107.6
14	CH2	−7.0	−4.9	−5.3	−4.0	−4.8	8.6
15	CH	−17.5	−16.0	−16.3	−14.9	−15.9	17.2
15	CH2	28.2	18.3	17.0	13.2	18.6	21.9
16	CH	108.8	93.6	95.5	87.7	95.5	95.9
17	CN	−8.3	−9.2	−9.7	−8.9	−9.1	9.5
18	CH2	32.0	20.4	19.0	15.1	21.0	24.5
18	C1(3)	−14.4	−13.7	−14.1	−13.2	−13.6	14.5

[a] From ref 44. [b] This work.

and in solution (e.g., refs 42 and 43, where it was referred to as N06). In the next section we give just a flavor of its broad performances, whereas the body of the paper is devoted to hyperfine coupling constants, which are one of the main

Table 7. Theoretical and Experimental Hyperfine Coupling Constants (Gauss) of Nitrogen Nuclei

structure	Nitrogen (^{14}N)	6–31G(d)[a]	EPR-III[a]	TZVP[a]	N07D[b]	exp[a]	structure	Nitrogen (^{14}N)	6–31G(d)[a]	EPR-III[a]	TZVP[a]	N07D[b]	exp[a]
12	N	10.0	8.2	6.2	11.0	9.2	69	2N	12.0	10.1	9.3	11.7	13.9
19	N	4.8	3.6	2.7	4.8	3.5	70	2N	12.4	10.8	10.0	12.3	13.3
20	N	11.9	10.1	7.8	12.7	10.0	71	2N	16.6	17.1	17.0	17.4	17.0
21	N	−15.2	−12.5	−10.6	−15.7	14.8	72	2N	11.7	10.9	10.1	12.1	14.7
22	N	14.8	12.1	10.4	15.2	14.3	73	2N	29.8	30.8	30.8	31.3	35.9
23	N	15.0	12.5	10.7	15.4	14.3	74	2N	29.9	31.8	31.9	31.1	38.7
24	N	13.0	10.7	8.5	13.7	12.5	75	2N anion	8.1	6.6	5.8	8.0	7.8
25	N	14.8	11.8	9.9	15.3	14.0	75	2N cation	13.9	12.1	11.3	13.2	21.0
26	N	15.4	12.4	10.6	15.7	14.3	76	2N anion	8.6	6.7	6.2	7.6	8.0
27	N	−18.7	−15.0	−13.3	−17.9	19.6	76	2N cation	12.6	10.9	10.2	11.9	20.0
28	N	17.3	14.3	12.8	16.9	19.3	77	2N	8.9	7.2	6.4	8.7	8.2
29	N	18.4	15.6	14.0	18.8	20.7	78	2N	9.5	7.4	7.1	8.1	9.2
30	N	17.1	14.1	12.6	16.5	18.7	79	2N	9.1	6.9	6.5	7.1	8.6
31	N	18.4	15.7	14.2	18.1	20.8	80	2N anion	9.3	7.5	6.8	8.5	8.8
32	N	15.6	13.0	11.7	15.2	18.6	80	2N cation	31.0	33.1	34.0	33.4	31.4
33	N	16.6	13.9	12.6	16.2	18.7	81	N	25.3	23.8	23.2	24.6	25.6
34	N	18.4	15.7	14.4	18.2	20.2	82	N	−24.8	−22.6	−22.3	−19.7	26.0
35	N	18.7	16.1	14.7	18.6	20.2	83	N	24.8	22.0	22.0	26.3	25.4
36	N	13.2	11.4	10.3	13.2	20.1	84	N	27.5	26.2	25.6	22.1	26.6
37	N	17.5	14.4	13.0	17.0	19.1	85	N	22.3	20.2	19.7	21.0	23.8
38	N	17.0	14.0	12.5	16.4	20.0	86	N	24.0	21.6	21.3	21.9	27.0
39	N	17.5	15.1	13.8	17.3	19.5	87	N	30.0	30.1	29.8	31.1	33.3
40	N	26.8	26.7	25.8	28.2	30.2	88	N	31.3	31.7	31.5	32.2	32.5
41	N	22.0	21.4	20.5	22.9	25.1	89	N	28.8	29.1	28.7	30.0	30.5
42	N	19.3	18.3	17.4	19.7	21.6	90	N	30.5	30.5	30.3	31.2	32.2
43	N	17.2	14.8	13.5	17.1	19.2	91	N	30.3	29.8	29.6	30.3	30.7
44	N	20.9	19.5	18.3	22.1	25.0	92	N	30.8	31.1	30.9	32.2	31.3
45	N	10.3	8.3	6.3	11.1	10.2	93	N	30.5	31.0	30.7	31.6	31.1
46	N	10.8	8.4	6.5	11.4	9.6	94	N	28.0	28.3	28.0	29.1	31.6
47	N	10.8	8.5	6.6	11.2	11.3	95	N	29.9	29.7	29.5	30.6	32.2
48	N	11.0	8.6	6.7	11.2	10.0	96	N	30.5	30.8	30.6	31.6	30.7
49	N	29.1	32.4	33.7	32.4	28.0	97	N	31.5	31.9	31.8	32.8	32.6
50	N	30.5	33.6	35.0	33.7	28.0	98	N	28.6	29.1	28.7	30.1	30.0
51	N	12.0	10.3	8.5	12.4	8.8	99	N	31.2	31.6	31.5	32.6	31.6
51	N	12.6	11.1	10.9	10.9	11.7	100	N	31.0	30.9	30.8	31.9	32.0
52	N	11.1	8.7	7.3	10.6	9.6	101	N	30.3	31.0	30.7	35.3	32.0
52	N	12.4	11.7	11.0	12.4	11.5	102	N	31.5	32.1	31.9	32.9	31.5
53	N	11.3	8.7	7.5	10.6	9.6	103	N	30.3	31.0	30.8	32.0	30.9
53	N	11.6	10.6	10.0	11.0	11.1	104	N	30.0	30.4	30.1	31.4	31.1
54	N	9.8	8.7	7.5	10.6	10.0	105	N	32.1	33.1	33.0	34.1	32.6
54	N	11.3	8.7	7.9	9.6	11.7	106	N	32.2	32.6	32.5	33.5	32.4
55	N	12.5	10.3	8.9	12.5	11.7	107	N	29.0	29.6	29.2	30.4	31.0
55	N	11.2	9.9	9.4	10.9	10.5	108	N	6.5	6.6	4.7	8.4	10.6
56	N	10.9	8.5	7.2	10.1	10.6	109	N	−12.8	−11.1	−10.4	−9.8	11.9
56	N	7.9	7.0	6.1	7.5	10.6	110	N	13.3	11.9	11.1	11.9	13.8
57	2N	12.0	9.8	8.8	10.7	11.6	111	N	15.0	14.0	13.0	15.0	15.2
58	2N	12.2	10.1	9.2	11.5	14.7	112	N	14.8	13.6	12.6	14.8	16.7
59	2N	12.5	10.5	9.6	11.8	13.0	113	N	12.3	11.1	10.0	12.2	15.9
60	N	15.7	13.9	12.7	15.7	16.1	114	N	13.9	12.7	11.8	14.2	16.2
60	N	10.8	8.7	8.1	9.7	9.7	115	N	13.3	11.9	10.9	12.9	14.9
61	2N	12.4	10.4	9.5	12.1	13.4	116	N	10.7	9.4	8.3	11.6	14.4
62	2N	11.1	9.3	8.4	10.8	13.2	117	N	13.6	12.3	11.4	13.8	15.2
63	2N	13.2	11.3	10.5	11.1	15.0	118	N	14.1	12.5	11.5	11.3	14.1
64	2N	12.5	10.6	9.7	11.1	15.0	119	N	−17.6	−17.1	−16.7	−21.6	19.8
65	2N	13.2	11.5	10.7	13.1	14.8	120	N	10.1	8.9	7.7	10.7	16.6
66	2N	11.4	9.5	8.6	11.2	12.9	121	N	17.1	16.8	15.9	15.0	16.9
67	2N	16.5	15.5	14.8	17.5	17.6	122	N	14.1	12.9	12.0	14.3	16.2
68	2N	15.0	14.0	13.3	15.7	16.0	123	N	14.2	12.9	12.0	14.3	14.5

[a] From ref 46. [b] This work.

targets of the present development. In this context, a recent systematic study by Hermosilla et al.[44–46] allows for the comparision of the performances of the B3LYP functional for a large set of hyperfine coupling constants employing several basis sets including 6–31G(d),[24] EPR-II,[38] EPR-III,[39] TZVP,[47] and cc-pVQZ.[48] Here we will show that much improved results are consistently obtained by the new N07D basis set with the same functional. As an aside, we have carefully selected a quite large set of experimental data, which represents, in our opinion, a useful benchmark for functional and/or basis set validation.

Computational Details

All the calculations were carried out by the Gaussian03 package[49] using the B3LYP hybrid density functional[41] with the N07D basis set. As mentioned in the Introduction, this basis set was obtained adding to a double-ζ description of

Table 8. Theoretical and Experimental Hyperfine Coupling Constants (Gauss) of Oxygen Nuclei

structure	Oxygen (^{17}O)	6–31G(d)[a]	EPR-III[a]	TZVP[a]	cc-pVQZ[a]	N07d[b]	exp[a]
3	O	11.1	9.9	10.2	9.5	10.4	6.6
7	O	−11.6	−12.5	−10.5	−8.1	−14.1	15.1
87	O	−18.1	−17.9	−14.1	−9.8	−21.2	22.8
123	O					−18.0	19.3
124	O	−0.2	−4.2	−4.1	−4.6	−3.5	5.0
125	O	−18.3	−15.7	−8.6	−1.5	−22.0	18.3
126	2O	−15.1	−13.9	−10.3	−5.8	−17.3	19.6
127	O	−31.0	−23.1	−16.0	−8.5	−29.3	29.7
128	2O	−14.5	−19.4	−16.9	−14.6	−20.3	21.8
129	O					−11.2	10.2
188	O			−2.2	−1.4	−3.5	3.6
199	O					−15.0	15.5

[a] From ref 44. [b] This work.

Table 9. Theoretical and Experimental Hyperfine Coupling Constants (Gauss) of Fluorine Nuclei

structure	Fluorine (^{19}F)	6–31G(d)[a]	EPR-III[a]	TZVP[a]	cc-pVQZ[a]	N07D[b]	exp[a]
9	F	−73.2	−52.2	−51.3	−44.7	−61.3	64.3
10	2F	−71.8	−77.2	−72.9	−62.4	−79.0	84.2
11	3F	133.9	138.3	133.4	125.6	134.5	142.4
130	F	71.1	92.0	84.8	91.4	86.2	81.7
131	F	47.0	31.0	29.5	19.6	31.5	32.6
134	2Feq	59.8	52.7	51.8	50.7	51.0	60.0
135	F	−14.1	−11.2	−12.4	−10.7	−12.6	8.0
136	4Feq	211.5	187.0	182.2	172.7	186.1	206.6
200	F		21.9			24.7	25.8
201	F1		−6.2			−6.7	4.8
201	F2,6		21.4			25.8	25.8
201	F3,5		22.8			24.2	25.8
202	F		15.9			17.7	16.2
203	F1,4		18.8			20.7	19.5
203	F2,3		4.0			4.5	6.5
204	F1,4		6.4			7.8	6.1
204	F2,3		2.7			2.7	2.1
205	F1		13.6			15.1	16.1
205	F3		6.0			6.9	7.1
205	F4		17.3			19.3	16.1
205	F5		17.9			19.8	16.8
205	F8		14.1			16.1	16.1
206	F1,5		15.1			16.7	17.9
206	F3,7		8.7			9.8	10.3
206	F4,8		15.5			17.3	17.9
207	F1,4,5,8		16.4			18.2	19.0
207	F2,3,6,7		3.3			3.8	4.8
208	F1,4		4.2			4.8	4.5
208	F2,3		2.5			2.5	2.3

[a] From ref 44 for 9, 10, 11, 130, 131; from ref 45 for 134, 135, 136, and from ref 55 for 200–208. [b] This work.

valence orbitals single sets of optimized core-valence *s* (on all atoms except H), diffuse *p* (on all atoms except H), polarization (on all atoms), and diffuse *d* (on O, F, Cl atoms) functions (Table 1). The inner electrons of second- and third-row atoms were described by the 6G basis set.[24]

Geometry optimizations and evaluations of harmonic frequencies have been performed in the gas phase using analytical gradients and Hessians. Nuclear hyperfine tensors have been computed following well-defined procedures described in recent literature.[32,50]

The hyperfine coupling tensor ($\boldsymbol{A}_X$), which describes the interaction between the electronic spin density and the nuclear magnetic momentum of nucleus *X*, can be split into three terms: $\boldsymbol{A}_X = a_X\boldsymbol{I}_3 + \mathbf{T}_X + \boldsymbol{\Lambda}_X$, where $\boldsymbol{I}_3$ is the 3 × 3 unit matrix. The first term (a_X), usually referred to as the Fermi-contact interaction, is an isotropic contribution, also known as a hyperfine coupling constant (hcc), and is related to the spin density at the corresponding nucleus *X*. The second contribution ($\boldsymbol{T}_X$) is anisotropic and can be derived from the classical expression of interacting dipoles. The last term, $\boldsymbol{\Lambda}_X$, is due to second-order spin–orbit coupling and can be determined by methods similar to those used for the *g*-tensor.[51] In the present case, because of the strong localization of spin density on the studied atoms and of their small spin–orbit coupling constants, its contribution can be safely neglected and will not be discussed in the following. Of course, upon complete averaging by rotational motions, only the isotropic part survives.

Results and Discussion

The N07D basis set has been assessed by comparison with some standard basis sets for a number of properties: a) geometrical parameters, b) dipole moments, and c) hyperfine coupling constants. Our results are collected in Tables 2−16

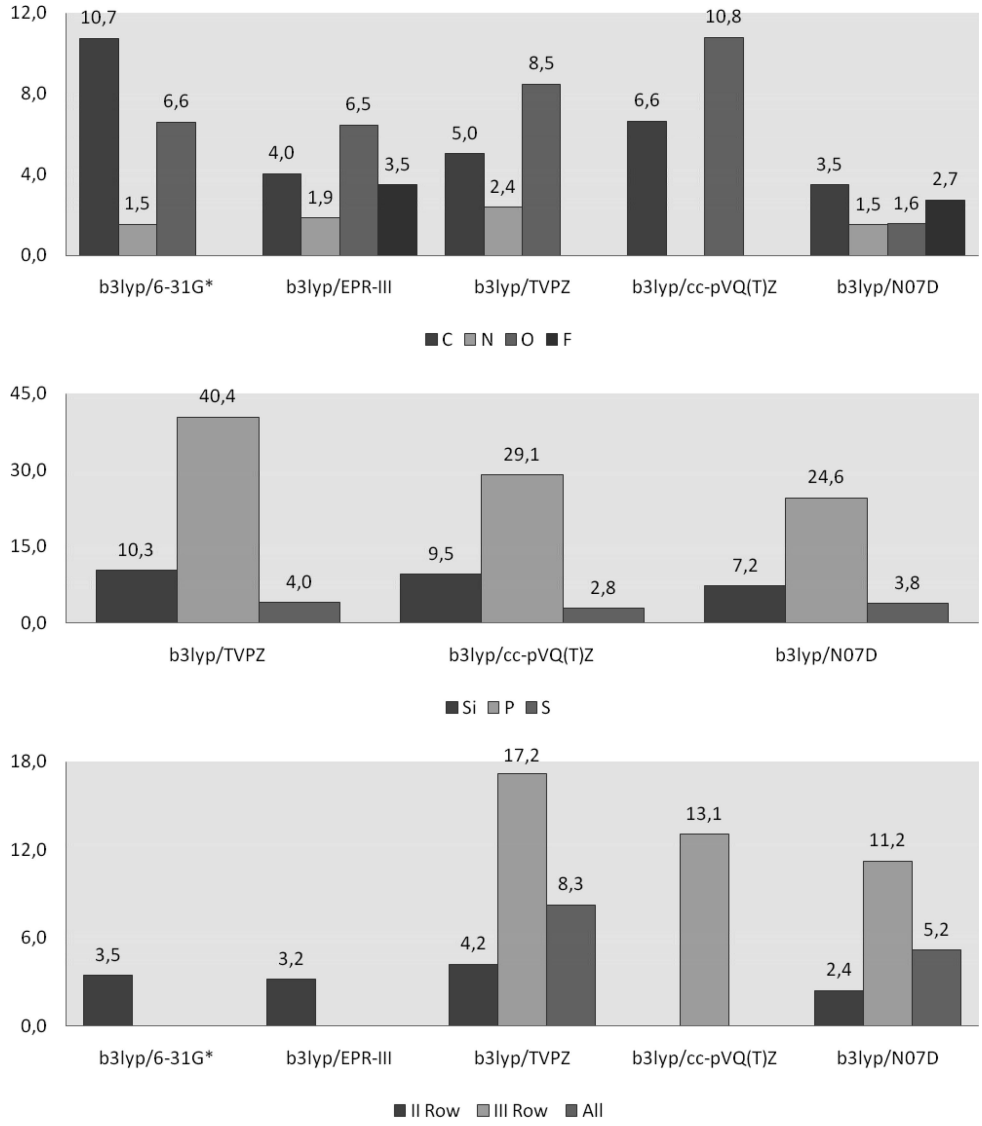

Figure 3. MADs (in Gauss) for nuclei of second and third rows. MAD (mean absolute deviation = $\Sigma|a_{calc}-a_{exp}|/N$).

and compared with other available theoretical and experimental results.

Before discussing the results in some detail, let us point out that for medium size basis sets (e.g., 6–31G(d,p), cc-pVDZ, N07D) the number of components of *d* functions plays an important role in obtaining accurate hyperfine coupling constants: in particular it is mandatory to use the redundant set of six *d* functions (which is the standard for 6–31G-like basis sets) because the additional *s* function implicitly added when using a 6d set plays a non-negligible role in completing the *s* space. Although this is not the case for larger basis sets (essentially equivalent results are obtained by the EPR-III basis set using 5d or 6d functions),[32,46] we think that this is a modest price to be paid for the much reduced cost of N07D wrt EPR-III. From another point of view, diffuse polarization functions play a significant role for electric properties, which are, in turn, related to noncovalent interactions. As a compromise between accuracy and cost, we decided, on the ground of test computations (some of which are discussed in the next section) to add diffuse *d* functions only on O, F, and Cl atoms.

Geometric Parameters and Electric Properties. The performances of the N07D basis set are generally comparable to those of aug-cc-pVDZ, with increased computational efficiency. For purposes of illustration, we report in Table 2 some significant parameters of H_2O, HF, HCl, and of the nitroxide radical TEMPO (Figure 1).[52–56] While structural parameters are generally satisfactory, irrespective of the presence of diffuse functions on O, F, and Cl atoms, dipole moments are significantly improved by the addition of diffuse polarization functions, reaching quantitative agreement with experiment. Thus the range of application of the B3LYP/N07D model is significantly enlarged by addition of diffuse polarization functions on electronegative atoms.

Hyperfine Coupling Constant. A variety of molecules containing hydrogen and atoms from the second- and third-row of the periodic table have been studied. We have taken 199 radicals (for a total of 221 hcc's) considered by Hermosilla and co-workers,[44–46] together with 9 additional radicals containing fluorine atoms.[57] The selected set (shown in Figure) includes neutral, cationic, anionic, doublet, triplet, quartet, localized, and conjugated radicals.

Table 10. Theoretical and Experimental Hyperfine Coupling Constants (Gauss) of Silicon Nuclei

structure	Silicon (^{29}Si)	TZVP[a]	cc-pVQZ[a]	N07D[b]	exp[a]
132	Si	−457.1	−456.9	497.9	498.0
138	Si	−391.8	−404.0	426.8	416.0
139	Si	−162.7	−161.4	164.6	181.0
140	Si	−275.7	−280.7	290.8	295.0
141	Si	−161.3	−160.2	164.2	183.0
142	Si	−159.8	−158.7	162.6	181.0
143	Si	−303.0	−305.8	311.0	339.0
144	Si	−145.5	−144.1	147.6	170.0
145	Si	−121.1	−125.3	122.9	137.0
146	Si	1.5	1.6[a]	−1.6	1.5
147	Si	6.8	7.5[a]	−7.1	7.0
148	2Si	6.6	7.9[a]	−5.6	6.7
149	2Si	6.1	6.6[a]	−5.6	5.7
150	Si	1.3	1.2[a]	−1.5	1.5
151	2Si	5.0	5.8[a]	−3.8	4.5
152	Si	5.8	6.7[a]	−4.9	6.2
153	2Si	4.2	4.2[a]	−4.3	3.9
154	Si	−140.4	−143.0[a]	137.5	163.0
155	Si	−62.8	−63.3[a]	53.9	64.0
155	3Si	4.0	3.4[a]	−4.9	7.1
156	2Si	5.2	5.4[a]	−5.1	4.6
157	2Si	3.9	4.0[a]	−3.9	3.5
158	2Si	2.9	3.3[a]	−3.5	2.7
159	4Si	−18.7	−19.1[a]	19.8	20.9
160	4Si	−9.8	−10.0[a]	10.2	12.5

[a] From ref 45. [b] This work.

Table 11. Theoretical and Experimental Hyperfine Coupling Constants (Gauss) of Phosphorus Nuclei

structure	Phosphorus (^{31}P)	TZVP[a]	cc-pVQZ[a]	N07D[bb]	exp[a]
131	P	96.9	72.1	65.1	84.8
133	P	702.6	701.9	728.4	721.3
134	P	1203.3	1241.8	1305.8	1330.0
135	P	−47.8	−41.9	−46.9	39.1
136	P	1262.3	1290.5	1427.6	1328.2
161	P	76.9	60.2	64.8	77.4
162	P	61.8	56.4	46.0	68.3
163	P	720.6	761.1	784.9	833.5
164	P	479.5	487.8	536.7	519.3
165	P	1248.5	1314.2	1312.9	1371.0
166	P	−12.5	−8.7	−15.7	13.5
167	P	−12.7	−9.2	−17.7	16.8
168	P	−12.5	−8.3	−16.5	14.7
169	P	302.2	319.5	317.4	375.0
170	P	322.1	322.2	329.1	388.9
171	P	469.1	475.2	495.1	484.0
172	P	22.4	19.8	18.5	23.6
173	P	61.9	70.7	72.2	78.7
174	P	297.3	312.9	318.5	361.6
175	2P	439.5	459.2	479.9	482.0
176	P	508.7	530.4	547.6	557.0

[a] From ref 45. [b] This work.

Before considering detailed results, we point out that the reduced number of experimental data available for Be, B, and Cl does not allow for a significant statistical analysis: the corresponding results are thus collected in Table 3 for purposes of illustration only: it is quite apparent that the N07D basis set delivers in all cases reasonable results.

For all the other atoms, we report the number of data (N), mean absolute deviation (MAD), data range, average absolute error, and mean percent error (MPE) between calculated and experimental values. Next we give the correlation coefficient (R^2), slope, and intercept of the least-squares line. The MAD and MPE only consider the absolute value, so that all

Table 12. Theoretical and Experimental Hyperfine Coupling Constants (Gauss) of Sulfur Nuclei

structure	Sulfur (^{33}S)	TZVP	cc-pVQZ	N07D[b]	exp
137	S	314.3	335.7	329.3	362.6
177	S	7.8	7.5	6.6	8.0
178	2S	3.4	3.2	3.2	4.2
179	2S	2.2	2.1	2.1	3.3
180	2S	3.4	3.1	3.2	4.4
181	2S	2.1	2.0	3.4	1.3
182	2S	7.9	7.1	6.9	9.8
183	2S	3.1	2.7	2.8	3.9
184	S	61.2	65.8	64.6	83.2
185	4S	3.5	3.2	3.0	4.3
186	4S	3.5	3.1	3.0	4.2
187	2S	7.6	6.4	6.5	9.4
187	2S	−0.8	−0.8[a]	−0.8	0.8
188	S2,6	−1.0	−1.1[a]	−0.8	1.4
189	2S	5.2	5.9[a]	4.2	7.2
190	S1,2,5,6	3.6	4.2[a]	3.1	4.4
191	S	8.4	9.3[a]	7.2	11.9
192	2S	7.1	7.8[a]	6.0	9.2
193	2S	4.4	5.0[a]	3.9	5.3
194	S	6.2	6.9[a]	5.4	8.3
195	4S	3.3	3.7[a]	2.8	4.1
196	4S	3.2	3.6[a]	2.7	4.0
197	2S	4.1	4.5[a]	3.5	4.6
198	4S	2.4	2.9[a]	2.1	3.4

[a] From ref 45. [b] This work.

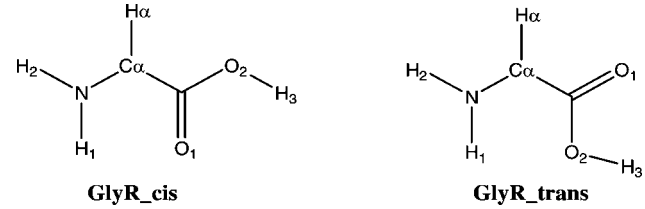

Figure 4. Structures of the glycine radical.

deviations are converted to positive numbers, added, and then averaged. Since the absolute errors increase, of course, with the range spanned by the corresponding hcc's, the error expressed in a percentage basis would seem coherent and intuitive: however, this procedure gives rise to serious difficulties with hcc's that are very small or close to zero. In such circumstances, regression analysis represents, in our opinion, the simplest and most useful approach for an unbiased comparison between large sets of computed and experimental hcc's.

Hydrogen atoms require some specific considerations in view of the lack of inner shells and of the overwhelming role of small hcc's in an unbiased statistics. We have thus selected a specific set of data in which the presence of σ radicals (characterized by large hcc's) has been overemphasized. The results collected in Tables 4 and 5 show that different basis sets are nearly equivalent in this connection leading to a percent error around 10%, which is close to that of second-row atoms.

We analyze the data for the other atoms in separate parts. In the first one, we consider each nucleus separately; next, atoms belonging to the same row of the periodic table are grouped together, and, finally, all the atoms are taken as a single set. We compare our results (Tables 6−12) with both experimental data and theoretical ones making explicit reference, in the latter case, to the B3LYP results with

Table 13. Data Analysis for Second Row Nuclei[a]

	6–31G(d)	EPR-III	TVPZ	cc-pVQZ	NO7D	exp
Carbon: $N = 23$						
MAD	10.7	4.0	5.0	6.6	3.5	
max absolute error	66.0	16.7	28.7	14.8	9.3	
average *E*%	18.6%	10.9%	9.3%	18.7%	10.5%	
max *E*%	74.8%	42.7%	38.0%	53.2%	43.9%	
R2	0.9915	0.9988	0.9991	0.9983	0.9991	
intercept	7.5938	−1.7012	−3.6841	−6.2305	−1.1153	
slope	0.9033	1.0182	1.0562	1.0196	0.9987	
max	495.3	569.3	587.8	566.5	555.3	561.3
min	2.7	4.9	5.3	4.0	4.8	8.6
Nitrogen: $N = 105$						
MAD	1.5	1.9	2.4		1.5	
max absolute error	6.5	7.7	8.9		5.9	
average *E*%	7.9%	10.3%	13.5%		8.1%	
max *E*%	39.2%	46.4%	55.7%		35.4%	
R2	0.9725	0.9751	0.9740		0.9771	
intercept	−2.2515	−4.6346	−6.3376		−3.8563	
slope	1.0314	1.1170	1.1639		1.1270	
max	32.2	33.1	33.0		35.3	33.3
min	6.5	6.6	4.7		8.4	10.6
Oxygen: $N = 12$						
MAD	6.6	6.5	8.5	10.8	1.6	
max absolute error	19.3	19.3	19.3	21.2	3.8	
average *E*%	33.6%	22.7%	38.8%	52.7%	16.4%	
max *E*%	96.0%	50.0%	54.5%	91.8%	57.7%	
R2	0.7982	0.9190	0.7383	0.2041	0.9359	
intercept	−1.1787	2.7574	2.8204	3.7203	1.0446	
slope	0.9311	0.6806	0.4738	0.2128	0.9246	
max	31.0	23.1	16.9	14.6	29.3	29.7
min	0.2	4.2	2.2	1.4	3.5	3.6
Fluorine: $N = 29$						
MAD		3.5			2.7	
max absolute error		19.6			20.5	
average *E*%		14.6%			12.4%	
max *E*%		40.0%			20.3%	
R2		0.9914			0.9956	
intercept		0.0117			1.6564	
slope		0.9320			0.9145	
max		187.0			186.1	206.6
min		2.5			2.5	2.1

[a] MAD (mean absolute deviation in Gauss) = $\Sigma|a_{calc}-a_{exp}|/N$(total nuclei); *E*% (percent error) = $a_{calc} - a_{exp}/a_{exp}$.

different basis sets reported in refs 44−46 and to some new EPR-III computations for aromatic radicals containing fluorine atoms. Tables 13−16 collect the results of the different statistical analyses, and Figure 3 sketches the MADs for each atom.

For the radicals containing carbon and oxygen atoms we compare our data with the theoretical ones calculated with four different basis sets [6–31G(d), EPR-III, TVPZ, and cc-pVQZ], whereas for nitrogen we have three basis sets [6–31G(d), EPR-III, and TVPZ] and for fluorine just one [EPR-III]. In general, all DFT methods yield a_X values close to the experimental ones, and the best results are consistently delivered by the N07D basis set. The performances of the different basis sets are compared in Figure 3 (MADs) and in Tables 13−15 (statistical analysis data). The N07D results for carbon and oxygen atoms are much better than those delivered by other (even significantly larger) basis sets both in terms of MADs (3.5 and 1.6 Gauss, respectively) and closeness of the slope of the linear regression to the theoretical value of 1.0 (0.999 and 0.925, respectively). The comparison for fluorine atoms is restricted to the EPR-III basis set due to the lack of other results: also in this case the N07D MAD is significantly better (2.7 vs 3.5 Gauss). As previously pointed out,[44] the 6–31G(d) basis set delivers particularly good results for nitrogen (albeit still inferior to their N07D counterparts), but this good behavior does not extend to other atoms, and, as said before, the geometries and interaction energies delivered by this basis set are not fully satisfactory. The B3LYP/N07D model gives by far the lowest MAD (Figure 3) for the whole set of C, N, O, F hcc's (2.4 Gauss). Moreover, the results of a linear regression for all nuclei of the second row (155), summarized in Table 8, shows that with N07D R^2 is higher (0.997) than with all the other basis sets, the slope is close to 1.0 (0.991), and the intercept is quite small (−0.873 Gauss).

For the third-row atoms, previous results have been obtained only with the TVPZ and cc-pVQZ basis sets, due to the lack of purposely tailored (e.g., EPR-III) basis sets. Except for the sulfur atom, for which the lowest MAD value is obtained with the cc-pVQZ basis set (2.8 vs 3.8 Gauss), N07D shows the best results (Figure 3). For all three atoms the R^2 value is higher than 0.99, and the slopes are considerably improved by using the N07D basis set and show values close to unit (Tables 7 and 8). The complete regression analysis performed for all third atoms indicates that the results are very satisfactory, indeed, the R^2 is 0.9958, the slope is 0.9956, and the MAD is the lowest among the available basis sets (Table 15). In summary, we can conclude

Table 14. Data Analysis for Third-Row Nuclei[a]

	TVPZ	cc-pVQZ	NO7D	exp
Silicon: $N = 25$				
MAD	10.3	9.5	7.2	
max absolute error	40.9	41.1	28.0	
average E%	10.6%	13.8%	11.1%	
max E%	43.7%	52.1%	31.7%	
R2	0.9988	0.9978	0.9955	
intercept	−1.0288	−0.9419	−4.0187	
slope	0.9166	0.9257	0.9803	
max	457.1	456.9	497.9	498.0
min	1.3	1.2	1.5	1.5
Phosphorus: $N = 21$				
MAD	40.4	29.1	24.6	
max absolute error	126.7	88.2	99.4	
average E%	11.5%	14.3%	10.8%	
max E%	24.4%	45.2%	32.7%	
R2	0.9968	0.9983	0.9942	
intercept	−3.3470	−10.7315	−13.1618	
slope	0.9196	0.9586	1.0060	
max	1262.3	1314.2	1427.6	1371.0
min	12.5	8.3	15.7	13.5
Sulfur: $N = 25$				
MAD	4.0	2.8	3.8	
max absolute error	48.3	26.9	33.3	
average E%	21.8%	19.2%	35.7%	
max E%	61.5%	53.8%	164.9%	
R2	0.9988	0.9989	0.9988	
intercept	−0.6699	−0.9042	−1.3765	
slope	0.8625	0.8952	0.9058	
max	314.3	335.7	329.3	362.6
min	0.8	0.8	0.8	0.8

[a] MAD (mean absolute deviation in Gauss) = $\Sigma|a_{calc}-a_{exp}|/N$(total nuclei); E% (percent error) = $a_{calc} - a_{exp}/a_{exp}$.

Table 15. Data Analysis for Second- and Third-Row and All Nuclei

	6–31G(d)	EPR-III	TVPZ	cc-pVQZ	NO7D	exp
II Row Atoms: $N = 155$						
MAD	3.5	3.2	4.2		2.4	
max absolute error	66.0	19.6	28.7		20.5	
average E%	12.9%	15.1%	20.4%		11.6%	
max E%	96.0%	50.0%	55.7%		57.7%	
R2	0.9903	0.9967	0.9955		0.9973	
intercept	1.1825	−2.6255	−4.3727		−0.8730	
slope	0.9364	1.0228	1.0544		0.9905	
max	495.3	569.3	587.8		555.3	561.3
min	0.2	3.6	2.7		3.5	3.5
III Row Atoms: $N = 71$						
MAD			17.2	13.1	11.2	
max absolute error			126.7	88.2	99.4	
average E%			14.7%	15.8%	19.1%	
max E%			61.5%	53.8%	164.9%	
R2			0.9979	0.9986	0.9958	
intercept			−1.7333	−3.7425	−5.8020	
slope			0.9171	0.9491	0.9956	
max			1262.3	1314.2	1427.6	1371.0
min			0.8	0.8	0.8	0.8
All Atoms: $N = 226$						
MAD			8.3		5.2	
max absolute error			126.7		99.4	
average E%			18.6%		14.0%	
max E%			61.5%		164.9%	
R2			0.9966		0.9963	
intercept			−1.1502		−2.1904	
slope			0.9246		0.9913	
max			1262.3		1427.6	1371.0
min			0.8		0.8	0.8

[a] MAD (mean absolute deviation in Gauss) = $\Sigma|a_{calc}-a_{exp}|/N$(total nuclei); E% (percent error) = $a_{calc} - a_{exp}/a_{exp}$.

that the B3LYP model couples computational efficiency and reliability for radicals involving atoms of the second and third row.

The performances of the B3LYP/N07D model for a typical problem involving at the same time stereoelectronic, vibrational, and environmental effects can be judged by the results

Table 16. Hyperfine Coupling Constants (in Gauss) of Glycine Radical

	exp	EPR-II average		N07D minimum		N07D average	
	pH: 1–10	cis	trans	cis	trans	cis	trans
N	6.4	5.5	5.5	4.1	4.1	6.3	6.3
H1	5.6	−5.4	−5.6	−7.7	−7.5	−5.3	−5.1
H2	5.6	−5.3	−5.4	−7.9	−7.7	−5.3	−5.1
Hα	11.8	−11.9	−11.7	−14.0	−14.1	−11.6	−11.7

reported in Table 16 for the glycine radical (GlyR, Figure 4) in aqueous solution.[43,58,59] Since the hcc's computed for the minimum energy structure in vacuum are significantly tuned by both intramolecular vibrations and by solvent librations, the reported results are obtained by averaging over 100 frames extracted at regular time steps from the ab initio dynamics described in ref 43. From a general point of view, all the computations provide, as expected, positive values for the C^{α} and N hcc's and negative values for the hydrogen atoms. Moreover, dynamical effects reduce the differences between the pairs H_1, H_2, and C^{α}, H^{α}. Polar solvents increase delocalization along the GlyR backbone, due to an increased importance of ionic resonance structures characterized by double N−C and C−C′ bonds and to the concomitant reduction of H^{α} hcc and of the pyramidalization of the aminic moiety. This last structural effect induces both a significant reduction of the H_2 hcc and an increased delocalization of the molecular orbital formally containing the unpaired electron, with the consequent reduction of the C^{α} and H^{α} hcc's. After averaging by MD in aqueous solution, the computed values are in general good agreement with experiment. It is, however, quite apparent that hydrogen atoms are described in a nearly equivalent way by the EPR-II and N07D basis set, whereas the nitrogen hcc is significantly improved by the new basis set, which is able to deliver quantitative agreement with experiment.

Concluding Remarks

Some hybrid functionals such as the popular B3LYP model are able to treat in a balanced way the differential spin polarization of different shells, thus providing a good description of the magnetic properties of many classes of compounds. Optimization of core-valence, diffuse, and polarization functions in a medium size basis set further extends the reliability of the computational model for both structural and magnetic properties. For all second-row atoms the B3LYP/N07D model couples quantitative agreement with experimental data and predictive power. The situation is slightly worse for third-row atoms, where recourse to regression analysis could prove valuable.

All in all, the B3LYP/N07D results seem accurate enough to allow for quantitative studies, especially taking into account that the same model and basis set can be used for different properties and for second- and third-row atoms. Furthermore, the availability of effective discrete/continuum solvent models and of different dynamical approaches, together with the reduced dimensions of the N07D basis set, allows for the performing of comprehensive analyses aimed at evaluating the roles of stereoelectronic, vibrational, and environmental effects in determining the overall properties of large flexible radicals of current biological and/or technological interest.

References

(1) Hill, J. G.; Platts, J. A.; Werner, H.-J. *Phys. Chem. Chem. Phys.* **2006**, *8*, 4072.

(2) Hobza, P.; Sponer, J. *Chem. Rev.* **1999**, *99*, 3247.

(3) Christiansen, O. *Theor. Chem. Acc.* **2006**, *116*, 106.

(4) Jurecka, P.; Sponer, J.; Cerny, J.; Hobza, P. *Phys. Chem. Chem. Phys.* **2006**, *8*, 1985.

(5) Barone, V.; Polimeno, A. *Chem. Soc. Rev.* **2007**, *36*, 1724.

(6) (a) Barone, V. *J. Chem. Phys.* **1994**, *101*, 10666. (b) Barone, V. *J. Chem. Phys.* **2005**, *122*, 014108.

(7) Adamo, C.; Barone, V. *J. Chem. Phys.* **1999**, *110*, 6158.

(8) Xu, X.; Goddard, W. A. *Proc. Natl. Acad. Sci. U.S.A.* **2004**, *101*, 2673.

(9) Zhao, Y.; Shultz, N. E.; Truhlar, D. G. *J. Chem. Theory Comput* **2006**, *2*, 364.

(10) Sato, S.; Tsuneda, T.; Hirao, K. *J. Chem. Phys.* **2007**, *126*, 234114.

(11) Tomasi, J.; Mennucci, B.; Cammi, R. *Chem. Rev.* **2005**, *105*, 2999.

(12) Brancato, G.; Barone, V.; Rega, N. *Theor. Chem. Acc.* **2007**, *117*, 1001.

(13) Scuseria, G. E. *J. Phys. Chem. A* **1999**, *103*, 4782.

(14) Benzi, C.; Improta, R.; Scalmani, G. *J. Comput. Chem.* **2002**, *23*, 341.

(15) Check, C. E.; Faust, T. O.; Bailey, J. M.; Wright, B. J.; Gilbert, T. M.; Sunderlin, L. S. *J. Phys. Chem. A* **2001**, *105*, 8111.

(16) Engels, B.; Peyerimhoff, S. D. *J. Phys. B* **1988**, *21*, 3459.

(17) Car, R.; Parrinello, M. *Phys. Rev. Lett.* **1985**, *55*, 2471.

(18) Schlegel, H. B.; Millam, J. M.; Iyengar, S. S.; Voth, G. A.; Daniels, D. A.; Scuseria, G. E.; Frisch, M. J. *J. Chem. Phys.* **2001**, *114*, 9758.

(19) Crescenzi, O.; Pavone, M.; de Angelis, F.; Barone, V. *J. Phys. Chem. B* **2005**, *109*, 445.

(20) Pavone, M.; Cimino, P.; De Angelis, F.; Barone, V. *J. Am. Chem. Soc.* **2006**, *128*, 4338.

(21) Iyengar, S. S.; Frisch, M. J. *J. Chem. Phys.* **2004**, *121*, 5061.

(22) Improta, R.; Barone, V.; Kudin, K. N.; Scuseria, G. E. *J. Am. Chem. Soc.* **2001**, *123*, 3311.

(23) Peterson, K. A.; Kendall, R. A.; Dunning, T. H. *J. Chem. Phys.* **1993**, *99*, 9790.

(24) Hariharan, P. C.; Pople, J. A. *Theor. Chim. Acta* **1973**, *28*, 213.

(25) Chipman, D. M. *Phys. Rev. A* **1989**, *39*, 475.

(26) Barone, V. *Theor. Chim. Acta* **1995**, *91*, 113.

(27) (a) Halls, M. D.; Schlegel, H. B. *J. Chem. Phys.* **1998**, *109*, 10587. (b) Halls, M. D.; Velkovski, J.; Schlegal, H. B. *Theor. Chim. Acc.* **2001**, *105*, 413.

(28) Barone, V. *J. Phys. Chem. A* **2004**, *108*, 4146.

(29) Huang, M. B.; Suter, H. U.; Engels, B.; Peyerimhoff, S. D.; Lunell, S. *J. Phys. Chem.* **1995**, *99*, 9724.

(30) Chipman, D. M. In *Quantum Mechanical Electronic Structure Calculations with Chemical Accuracy*; Ronghoff, S., Ed.; Kluwer: Amsterdam, 1995; p 109.

(31) Al Derzi, A. R.; Fau, S.; Bartlett, R. J. *J. Phys. Chem. A* **2003**, *107*, 6656.

(32) Improta, R.; Barone, V. *Chem. Rev.* **2004**, *104*, 1231.

(33) Barone, V.; Adamo, C.; Russo, N. *Chem. Phys. Lett.* **1993**, *212*, 5.

(34) Barone, V. *J. Phys. Chem.* **1995**, *99*, 11659.

(35) Schoneborn, J. C.; Neese, F. W.; Thiel, *J. Am. Chem. Soc.* **2005**, *127*, 5840.

(36) Mattar, S. M. *J. Phys. Chem. A* **2007**, *111*, 251.

(37) Kaprzac, S.; Reviakine, R.; Kaupp, M. *J. Phys. Chem. B* **2007**, *111*, 811.

(38) Adamo, C.; Cossi, M.; Barone, V. *THEOCHEM* **1999**, *493*, 145.

(39) Rega, N.; Cossi, M.; Barone, V. *J. Chem. Phys.* **1996**, *105*, 11060.

(40) Barone, V.; Cimino, P. *Chem. Phys. Lett.* **2008**, *454*, 139.

(41) Stephens, P. J.; Devlin, F. J.; Chabalowski, C. F.; Frisch, M. J. *J. Phys. Chem.* **1994**, *98*, 11623.

(42) Brancato, G.; Rega, N.; Barone, V. *Theor. Chem. Acc.* **2007**, *117*, 1001.

(43) Brancato, G.; Rega, N.; Barone, V. *J. Am. Chem. Soc.* **2007**, *129*, 15380.

(44) Hermosilla, L.; Calle, P.; Garcia de la Vega, J. M.; Sieiro, C. *J. Phys. Chem. A* **2005**, *109*, 114.

(45) Hermosilla, L.; Calle, P.; Garcia de la Vega, J. M.; Sieiro, C. *J. Phys. Chem. A* **2005**, *109*, 7626.

(46) Hermosilla, L.; Calle, P.; Garcia de la Vega, J. M.; Sieiro, C. *J. Phys. Chem. A* **2006**, *110*, 13600.

(47) Godbout, N.; Salahub, D. R.; Andzelm, J.; Wimmer, E. *Can. J. Chem.* **1992**, *70*, 560.

(48) Peterson, K. A.; Kendall, R. A.; Dunning, T. H. *J. Chem. Phys.* **1993**, *99*, 1930.

(49) *Gaussian 03, Revision D.02*; M. J. Frish, G. W. Truck, H. B. Schlegel, G. E. Scuseria, M. A. Robb, J. R. Cheeseman, J. A. Montgomery, Jr., T. Vreven, K. N. Kudin, J. C. Burant, J. M. Millam, S. S. Iyengar, J. Tomasi, V. Barone, B. Mennucci, M. Cossi, G. Scalmani, N. Rega, G. A. Petersson, H. Nakatsuji, M. Hada, M. Ehara, K. Toyota, R. Fukuda, J. Hasegawa, M. Ishida, T. Nakajima, Y. Honda, O. Kitao, H. Nakai, M. Klene,X. Li. J. E. Knox, H. P. Hratchian, J. B. Cross, C. Adamo, J. Jaramillo, R. Gomperts, R. E. Stratmann, O. Yazyev, A. J. Austin, R. Cammi, C. Pomelli, J. W. Ochterski, P. Y. Ayala, K. Morokuma, G. A. Voth, P. Salvador, J. J. Dannenberg, V. G. Zakrewski, S. Dapprich, A. D. Daniels, M. C. Strain, O. Farkas, D. K. Malick, A. D. Rabuck, K. Raghavachari, J. B. Foresman, J. V. Ortiz, Q. Cui, A. G. Baboul, S. Clifford, J. Cioslowski, B. B. Stefanov, G. Liu, A. Liashenko, P. Piskorz, I. Komaromi, R. L. Martin, D. J. Fox, T. Keith, M. A. Al-Laham, C. Y. Peng, A. Nanayakkara, M. Challacombe, P. M. W. Gill, B. Johnson, W. Chen, M. W. Wong, C. Gonzalez, J. A. Pople, Gaussian, Inc.: Wallingford, CT, 2004.

(50) Barone, V.; Cimino, P.; Pavone, M. In *Continuum Solvent Models in Chemical Physics: from Theory to Applications*; Mennucci, B., Cammi, R., Eds.; Wiley & Sons, Ltd.: 2007; Chapter *2.2*, pp 145–166.

(51) Neese, F. *J. Chem. Phys.* **2003**, *118*, 3939.

(52) Rustad, J. R.; Felmy, A. R.; Hay, B. P. *Geochim. Cosmochim. Acta* **1996**, *60*, 1553.

(53) Deyer, P. J.; Cummings, P. T. *J. Chem. Phys.* **2006**, *125*, 144519.

(54) Mason, M. G.; van Holle, W. G.; Robinson, D. W. *J. Chem. Phys.* **1971**, *54*, 3491.

(55) Werner, H. J.; Pavel, R. *J. Chem. Phys.* **1980**, *73*, 2319.

(56) Doerksen, R. J.; Thakkar, A. J.; Koga, T.; Hayashi, M. *THEOCHEM* **1999**, *488*, 217.

(57) Rakitin, A. R.; Yff, D.; Trapp, C. *J. Phys. Chem.* **2003**, *107*, 6281.

(58) Rega, N.; Cossi, M.; Barone, V. *J. Am. Chem. Soc.* **1997**, *119*, 12962.

(59) Rega, N.; Cossi, M.; Barone, V. *J. Am. Chem. Soc.* **1998**, *120*, 5723.

CT800034C